2018 IEEE 13th International Conference on Industrial and Information Systems (ICIIS)

Solar PV interface to Grid-Tie Inverter with Current Referenced Boost Converter

Gautam A. Raiker *, Subba Reddy B., Praveen C. Ramamurthy, L. Umanand, Abines S. G.†, Shama G. Vasisht‡
Interdisciplinary Center for Energy Research
Indian Institute of Science
Bangalore, 560012, India
*Email ID: gautamraiker@iisc.ac.in

***Abstract*—A Solar Photovoltaic (PV) array may be interfaced with the Grid-Tie Inverter (GTI) either by direct connection or through a Boost Converter. In case of direct connection of PV with GTI the string voltage has to be maintained at the specified DC link Voltage level according to the Maximum Power Point (MPP) and the input range of the GTI by connecting the required number of PV panels to the string. In this case the Maximum Power Point tracking is done by giving the current reference to the inverter control and the response of the tracking may be limited by the inner current loops. Instead we can use a Boost converter to perform the dual function of stepping up the voltage and tracking the maximum power point. A Current Referenced Boost Converter has been proposed in this work in which the control is PWM mode with current feedback. The plant model is derived and a PI controller is tuned to satisfy the performance and stability requirements. The current referenced controller works well for Partially Shaded conditions and also has the ability to control the PV power by operating the PV array at any current reference in case of excess energy generation.**

***Index Terms*—Photovoltaics (PV), Grid-Tie Inverter (GTI), Maximum Power Point Tracking (MPPT), Converter Modeling, Boost Converter, Momentum Term, Partial Shading.**

I. Introduction

In the present work a Space Vector based Pulse Width Modulated Grid Connected Inverter which is integrated with PV and battery energy storage system (BESS) has been modeled. Control systems have been developed for controlling power flow between the PV array, Inverter, Grid and the Battery. When PV is pumping current into the grid it should be free from harmonics, so the inverter is designed using Space Vector Modulation technique to reduce the harmonic content. The current injected into the grid must be in phase with the grid voltage and it should to be operated in ”Grid Following” mode. Therefore the control systems associated with the inverter is suitably designed to achieve this. Also the operating point of the PV is chosen in such a way that, maximum power is extracted from the PV panel. To achieve this a MPPT (Maximum Power Point Tracking) algorithm is used to keep the Q-point of the PV panel always near to the peak power point. PV being intermittent source cannot supply power at all times, so battery energy storage system (BESS) is used to aid the grid during peak loads. The battery could be charged by the PV and grid during non-peak loads. During peak loads, the charged battery also aids the grid along with PV.

The PV array is interfaced with the Grid-Tie Inverter (GTI) by a Current Referenced Boost Converter [1]. The PV current in a Current Referenced Boost converter can be commanded to any value as long as it is within the short circuit current level. This gives the option of either using the PV array in MPPT mode or in constant current operation at the desired current value. Another advantage of Current Referenced operation is that during Partial Shading condition since the IV curve current doesn’t fall completely to shaded level, the MPPT continues to track at the maximum power point without loosing control.

II. Small Signal Model of Boost Converter

In the small signal model the characteristics of the PV source needs to be included which is given by the dynamic resistance of the I-V characteristics as shown in (1).

$$r_{pv} = \frac{\mathrm{d}v}{\mathrm{d}i} \approx \frac{\tilde{v_{pv}}}{\tilde{i_{pv}}} \tag{1}$$

This dynamic resistance [2] is negative in value as it can be seen from the I-V characteristics of the PV source shown in Fig. 1. The I-V characteristics is be broken down into four portions: current source region, power source region 1, power source region 2 and voltage source region based on the dynamic resistance values in these regions.

The input current to duty cycle transfer function was found to be as shown in (2), where V_{DC} is the DC link voltage at the output of the Boost Converter, V_F is the forward voltage of the diode, R_L is the series resistance with the inductor (L) and C is the input side capacitance.

$$\frac{\tilde{i_L}}{\tilde{d}} = \frac{\left(\frac{V_{DC}+V_F}{R_L - r_{pv}}\right)\left(1+\frac{s}{\omega_z}\right)\omega_i^2}{s^2 + 2\zeta_i\omega_i s + \omega_i^2} \tag{2}$$

$$\omega_i = \sqrt{\frac{-r_{pv}+R_L}{-r_{pv}LC}} \tag{3}$$

$$\zeta_i = \frac{r_{pv}R_L C - L}{2\omega_i r_{pv} LC} \tag{4}$$

$$\omega_z = \frac{1}{-r_{pv}C} \tag{5}$$

† Summer Research Fellow under Indian Academy of Sciences at Indian Institute of Science, Bangalore. ‡ Summer Intern at Interdisciplinary Center for Energy Research, Indian Institute of Science, Bangalore.

TABLE I
OPEN LOOP PARAMETERS

Operating Point	$r_{pv}(\Omega)$	DC Gain (dB)	$\omega_i(rad/sec)$	ζ_i	$\omega_z(rad/sec)$
Current Source Region	-641.0	0.771	632.51	0.0214	3.100
Power Source Region 1	-30.14	27.29	633.71	0.0713	66.40
Power Source Region 2	-3.338	46.01	643.55	0.4773	590.3
Voltage Source Region	-1.476	52.85	657.66	1.0484	1.355×10^3

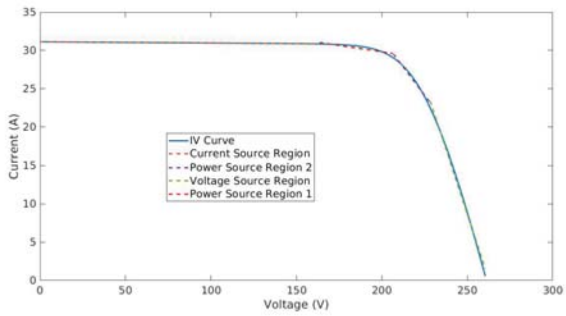

Fig. 1. Fitting of IV Curve in different regions.

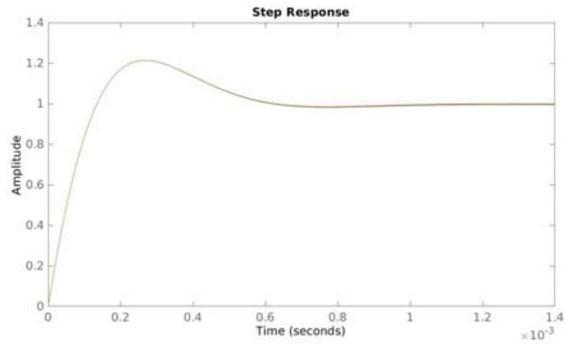

Fig. 3. Step Response of the Closed Loop Current Referenced Controller.

The open loop parameters of the small signal model are shown in Table 1. The parameters vary in the different zones which have been defined.

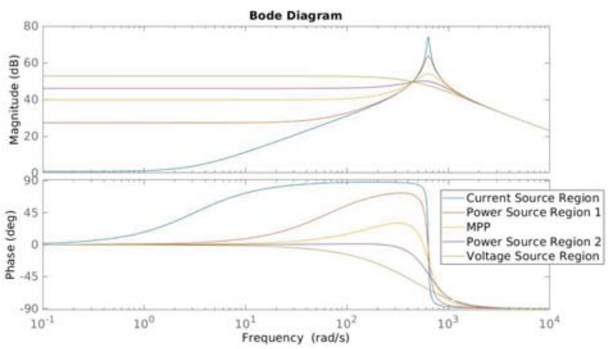

Fig. 2. Bode Plot for the different regions.

III. PI CONTROLLER

A standard Proportional Integral (PI) controller is utilized in order to have zero steady state error to step input in current and the required phase margin. The Open Loop Bode Plot Characteristics are shown for the different regions as in Fig. 2. The PI controller is designed to meet stability and steady state performance. The transfer function of the PI controller is shown in (6). The step response of the close loop system is shown in Fig. 3.

$$C(s) = 0.0806 + \frac{500}{s} \quad (6)$$

IV. PARTIAL SHADING EXPERIMENT

Two solar panels each rated at 40V, 250W were connected in series and one of them was under diffused sunlight ($250W/m^2$) and the other was at maximum irradiance of $900W/m^2$. Their IV and PV curve [9] was plotted as shown in Fig. 4. Seaward PV200 was used to record the data of the panel(V and I values from Voc to Isc). Irradiance was measured using Solar Survey 200R. The maximum power was found to be 163.4W at a MPP of 163.2V and 27.65A.

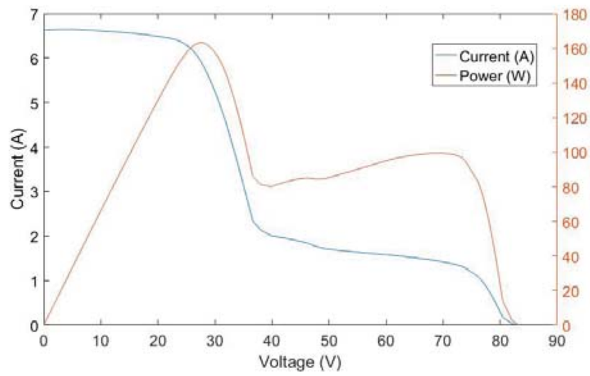

Fig. 4. Partially Shaded Condition, Experimental P vs V and I vs V curves.

The experimental results were verified by simulation in Simulink by keeping one panel at $1000W/m^2$ and other shaded at $200W/m^2$ as shown in Fig. 5.

V. SPACE VECTOR PWM

Conventional space vector PWM (CSVPWM) has the advantages of yielding up to 15% higher fundamental line-side

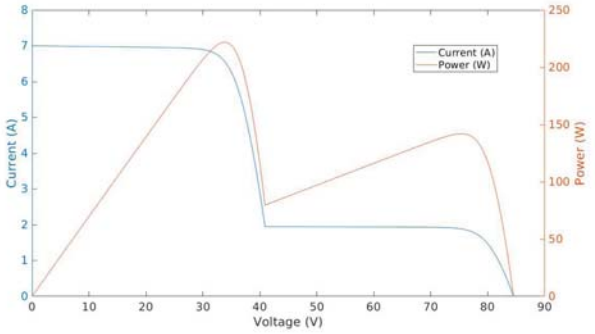

Fig. 5. Partially Shaded Condition, Simulated P vs V and I vs V curves.

voltage for a given DC bus voltage and also less harmonic distortion in line currents over sine-triangle PWM (SPWM) [6]. Space Vector PWM (SVPWM) is implemented using micro-controllers or DSPs. The simple digital implementation algorithm of SVPWM is given in reference [8]. Similar to SPWM, the modulating signal is compared with a high frequency triangle which may be a timer, increasing linearly. Through linear relations we can convert the amplitudes of the modulating signals V_a, V_b, V_c into time as T_a, T_b, T_c.

Algorithm for digital implementation is as follows:

- The following equations are calculated.

$$T_a = (T_s/V_{dc}) * V_a \tag{7}$$

$$T_b = (T_s/V_{dc}) * V_b \tag{8}$$

$$T_c = (T_s/V_{dc}) * V_c \tag{9}$$

  where T_s where is the subcycle period.
- Maximum of T_a, T_b, T_c is calculated and it is denoted as T_{max}.
- Minimum of T_a, T_b, T_c is calculated and it is denoted as T_{min}.
- T_{eff} is found by subtraction of T_{max} and T_{min}.
- $T_0 = T_s T_{eff}$ is calculated. Where T_0 is the Off time of switches.
- The offset which has to be added to T_a, T_b, T_c is calculated as T_{offset} which is given by $T_{offset} = T_{min} + T_0/2$.
- Therefore,

$$T_{aOn} = T_a + T_{offset} \tag{10}$$

$$T_{bOn} = T_b + T_{offset} \tag{11}$$

$$T_{cOn} = T_c + T_{offset} \tag{12}$$

- The above calculated values are stored in compare registers and it is compared with the value in the timer register.
- The timer is programmed in such a way that it starts from 0 and counts till T_s and then counts back from T_s to 0 again and repeats in the same fashion.

VI. Maximum Power Point Tracking

The MPPT algorithm used in the proposed model is Perturb & Observe [3] [4] . The PV panel current is first perturbed in a particular direction by perturbing reference current of the Boost Converter. If there is an increase in power, the subsequent perturbation should be kept in the same direction and if there is a decrease in power, the perturbation should be reversed. This is done repeatedly until we reach the maximum power point.

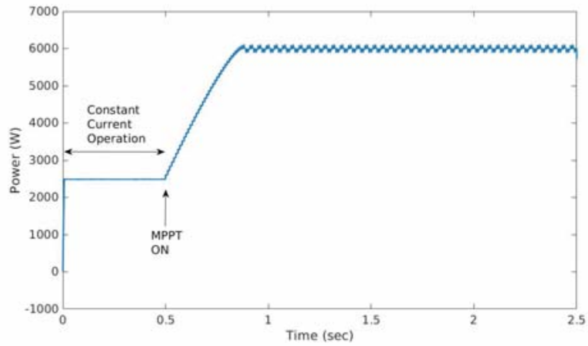

Fig. 6. Tracking of Power with Time.

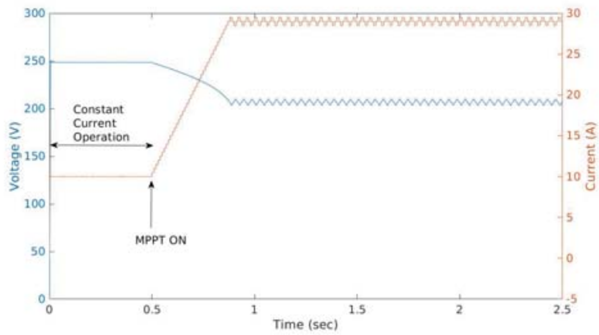

Fig. 7. Tracking of Current and Voltage Waveforms.

A Momentum term can be introduced in the perturbation similar to that used in gradient descent learning based back propagation algorithms for updating the weights of neural networks [5]. Let $\Delta I(n)$ be the current perturbation for instant 'n' shown in (7), which is given in terms of the previous perturbation $\Delta I(n-1)$ scaled by a factor α and the step size of the P&O method given by $f(n)$.

$$\Delta I(n) = \alpha \Delta I(n-1) + f(n) \tag{13}$$

This factor $\alpha \Delta I(n-1)$ is called as the momentum term. Addition of this term accelerates tracking when far away from the MPP and reduces the step size when MPP is reached. The step size in the simulation study is taken to be $0.5A$ and α was taken as 0.7. The tracking of the Power is shown in Fig. 6, and current and voltage waveforms are shown in Fig. 7. The step size of the P&O with momentum term increases dynamically until a steady state value when previous perturbations are in the same directions. The step size decreases as there are oscillations in previous perturbations. A more detailed analysis of this has been given in [5].

VII. Proposed Model of Grid-Tie Inverter

The system specifications are given in Table 2. As it can be seen from the block diagram in Fig. 10, there is a PV panel which is connected to a Boost converter which acts as power interface. The boost converter is connected to the Three Phase Inverter through a DC link capacitor. The inverter is connected to the grid via a filter. In the proposed model the grid is modeled as a three phase source. The three phase voltages and currents are sensed and are given to the respective control loops [7]. The PLL block ensures that the voltage and current are in phase. The current control loop is used to control the amount of current that is pumped into the inverter.

TABLE II
Specifications

System Specifications	
PV array	250Wp panels. 6 panels per string 4 strings in parallel Total=6000kWp
C_{pv}	$500\mu F$
L	5mH
C_{DClink}	$500\mu F$
Filter	20mH
Grid	$400V_{L-L}$
BESS	12V, 200Ah battery 24 per string 2 strings in parallel Total=9600Ah

The MPPT controller gives the value of current reference so that maximum power can be extracted from the PV panel. The PWM block generates gate pulses by Space Vector PWM (SVPWM) as described in the background section. These gate pulses drive the inverter to produce output voltage and current with lesser harmonic content. Further there is also a battery storage that is connected to the DC link capacitor through another boost converter. This battery storage aids the PV panel to supply the grid during peak demands.

The simulation results show that the current which is pumped into the grid is in phase with the grid voltage i.e. the model is injecting only real power into the grid. This is evident from Fig. 8.

The three phase output current of the grid-tie inverter is shown in Fig. 9. The MPPT turns on at 0.5sec and later at 2.5sec the insolation falls from $1000W/m^2$ to $500W/m^2$. There is a blanking period of about 0.5sec after the change in insolation occurs where the PV doesn't supply any power. This is because the reference current demanded is much larger that the actual current available when insolation drops. Hence MPPT looses control for a while till the reference current comes back to normal value. This has happened because we have given an instantaneous drop in insolation. Ideally the change in insolation will be gradual and such an occasion will not occur.

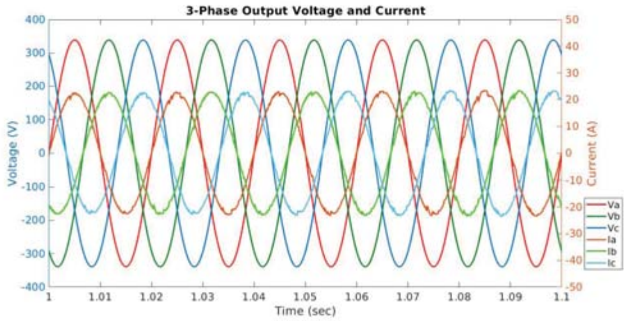

Fig. 8. Three Phase Output Voltage and Current.

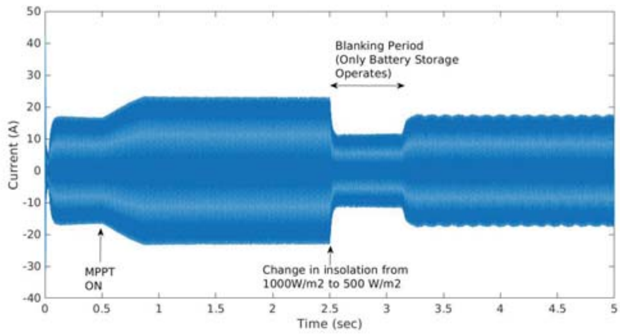

Fig. 9. Three Phase Current Waveforms.

VIII. Proposed Solution to Partial Shading

The current referenced Boost Converter presents a solution to the partial shading problem, when diffused sunlight falls on part of the Solar PV array. In Fig. 11 one half of the array falls under diffused sunlight at $200W/m^2$ and the remaining part has insolation of $1000W/m^2$. The global maximum power is 3000W as seen from the P vs V curve in Fig. 11 and the MPP is at 103V and 29A.

From Fig 12. and Fig. 13 it can be seen that the global maximum is tracked in the partial shading conditions. When the case of partial shading occurs we can see from the IV curve that the unshaded value of current at maximum power is around the same as the partially shaded current at maximum power which is around 29A. This is the reason why the current waveform remains basically constant when partial shading occurs whereas the voltage drops to take care of the drop in power as can be seen in Fig. 13. The global maximum is tracked because since the system is current referenced, during partial shading this current level is available and hence there is no blanking period where the MPPT looses tracking control. This example is of the case where the system is from full insolation to partially shaded.

The currents injected into the grid during the transition from full insolation to partially shaded condition can be can be

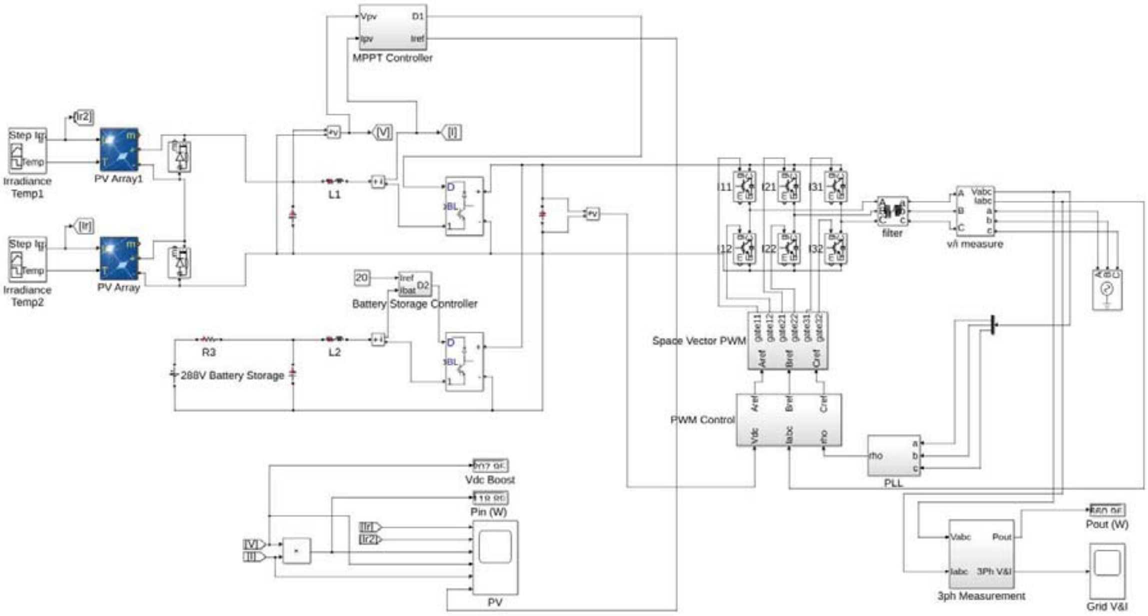

Fig. 10. Simulink Block Diagram of System.

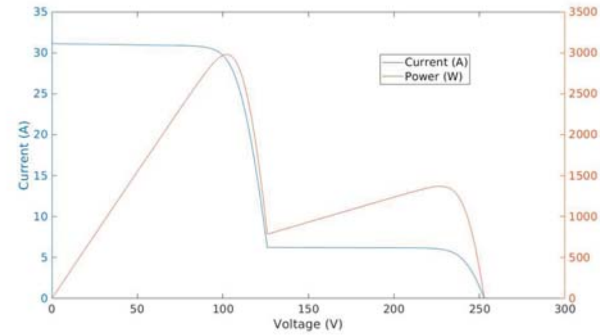

Fig. 11. I vs V and P vs V curves for the system under Partially Shaded Condition.

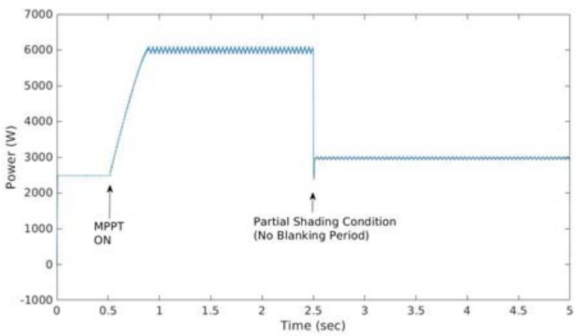

Fig. 12. Tracking of Power for the System under Partially Shaded Condition.

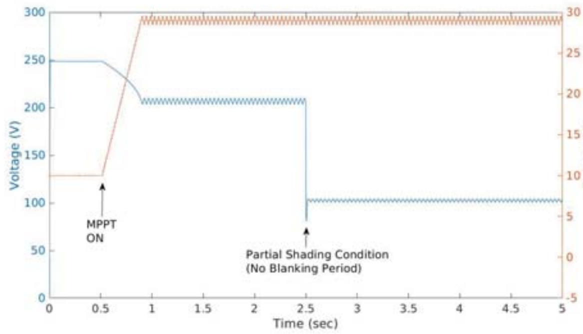

Fig. 13. Tracking of Voltage and Current for the System under Partially Shaded Condition.

seen in Fig. 14. There is a smooth transition without any kind of blanking period. It has to be noted though, that it is possible that in the unlikely case of fully shaded condition to partially shaded condition the MPPT may track to the local maximum. This is because the initial current will be low due to full shading and the tracking will proceed from there on. A condition to detect this case has to be defined and implemented in the MPPT. By detecting this condition and tracking the global maxima for this case the MPPT algorithm will be a solution for Partial Shading in any condition. Since such cases (transition from fully shaded to partially shaded) are rare and temporary the MPPT algorithm is kept simple in the proposed solution.

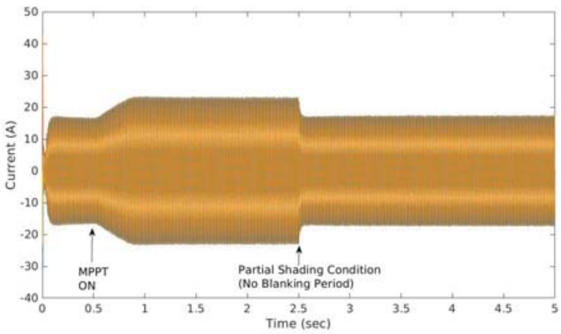

Fig. 14. Three Phase Current Waveforms under Partially Shaded Condition.

IX. Conclusions

The model developed successfully integrated Solar PV and BESS to the grid, through a Grid-Tie inverter. Maximum Power is pumped from the PV by operating in MPPT mode. Also any other power reference can be commanded by operating in current referenced mode. The MPPT algorithm used was Perturb and Observe with Momentum Term to accelerate tracking and reduce oscillations about MPP. The problem of partial shading in the case when transition happens from full insolation to partially shaded condition is inherently taken care by the current referenced MPPT algorithm. It has to be added that in case of rapidly changing insolation there may be a blanking period involved. Also to track MPP in all cases, a condition to detect the case of transition from fully shaded to partially shaded condition, has to be added in the MPPT algorithm.

Acknowledgment

This research is based upon work supported by the Department of Science and Technology (DST), the project entitled UK India Clean Energy Research Institute (UKICERI) (Sanction No. DST/RCUK/JVCCE/2015/02).

References

[1] S. Kouro, J. I. Leon, D. Vinnikov and L. G. Franquelo, “Grid-Connected Photovoltaic Systems: An Overview of Recent Research and Emerging PV Converter Technology,” in IEEE Industrial Electronics Magazine, vol. 9, no. 1, pp. 47-61, March 2015.

[2] W. Xiao, W. G. Dunford, P. R. Palmer and A. Capel, “Regulation of Photovoltaic Voltage,” in IEEE Transactions on Industrial Electronics, vol. 54, no. 3, pp. 1365-1374, June 2007.

[3] N. Femia, G. Petrone, G. Spagnuolo, and M. Vitelli, “Optimization of perturb and observe maximum power point tracking method,” IEEE Transactions on Power Electronics, vol. 20, no. 4, pp. 963973, July 2005.

[4] N. Femia, G. Petrone, G. Spagnuolo, and M. Vitelli, Power Electronics and Control Techniques for Maximum Energy Harvesting in Photovoltaic Systems. Boca Raton: CRC Press, 2013.

[5] G. A. Raiker, “Dynamic response of maximum power point tracking using perturb and observe algorithm with momentum term,” 2017 IEEE 43rd Photovoltaic Specialists Conference (PVSC), June 2017, to be published.

[6] P. Srikant Varma, G. Narayanan, “Space vector PWM as a modified form of sine-triangle PWM for simple analog or digital implementation,” IETE Journal of Research, vol. 52, no. 6, pp. 435-449, 2006.

[7] J. S. Siva Prasad, T. Bhavsar, R. Ghosh, and G. Narayanan, “Vector control of three-phase AC/DC front-end converter,” Sadhana, vol. 33, no. 5, pp. 591-613, October 2008.

[8] L. Umanand, Power Electronics: Essentials & Applications. Wiley India, 2010.

[9] H. Patel and V. Agarwal,“MATLAB-Based Modeling to Study the Effects of Partial Shading on PV Array Characteristics,” in IEEE Transactions on Energy Conversion, vol. 23, no. 1, pp. 302-310, March 2008.